the structure to meet the example criteria. It has been demonstrated that existing methodology is sufficient to permit damage tolerance criteria to be formally considered in the design of primary aircraft structure. The results of the application study indicate that by proper choice of material and design concept, aircraft structure can be designed to meet damage tolerance criteria with little or no weight penalty.

References

[1]Ekvall, J. C., Brussat, T. R., Liu, A. F., and Creager, M., "Engineering Criteria and Analysis Methodology for the Appraisal of Potential Fracture Resistant Primary Aircraft Structure," AFFDL-TR-72-80, Sept. 1972, Air Force Flight Dynamics Lab., Wright-Patterson Air Force Base, Ohio.

[2]Brussat, T. R., "An Approach to Predicting the Growth to Failure of Fatigue Cracks Subjected to Arbitrary Uniaxial Cyclic Loading," *Damage Tolerance in Aircraft Structures,* ASTM STP 486, May 1971, American Society for Testing and Materials, Philadelphia, Pa., pp 122–143.

[3]Emero, D. H. and Spundt, L., "Optimization of Multirib Wing Box Structures Under Shear and Moment Loads," AIAA 6th Structures and Materials Conference, April 1965, Palm Springs, Calif.

[4]Brussat, T. R., "Rapid Calculation of Fatigue Crack Growth by Integration," presented at the 7th National Symposium on Fracture Mechanics, College Park, Md., Aug. 27–29, 1973.

[5]Poe, C. C., Jr., "Fatigue Crack Propagation in Stiffened Panels," *Damage Tolerance in Aircraft Structures,* ASTM STP 486, May 1971, American Society for Testing and Materials, Philadelphia, Pa., pp 79–97.

[6]Vlieger, H. "Residual Strength of Cracked Stiffened Panels," NLR-TR-71004U, Jan. 1971, National Aerospace Laboratory, The Netherlands.

[7]Crichlow, W. J., "The Ultimate Strength of Damaged Structure—Analysis Methods with Correlating Test Data," in *Full-Scale Fatigue Testing of Aircraft Structures,* Pergamon Press, New York, 1960, pp. 149–209.

MARCH 1974 J. AIRCRAFT VOL. 11, NO. 4

Gradient Optimization of Structural Weight for Specified Flutter Speed

E. E. Simodynes*
General Dynamics, Fort Worth, Texas

A method for optimizing structures to satisfy flutter requirements is presented. The specific algorithm employs a gradient of total weight with respect to variable structural parameters as the specified flutter speed remains constant. Equations are derived for direct calculation of the gradient. In applications thus far, the method has been efficient in reducing structural weight while retaining flutter speed without frequent recalculation of normal modes of vibration. An all-movable horizontal tail application is cited in which the skin alone and then the entire structure is resized. Applications using 2 and 6 modes of vibration are also compared.

Introduction

A USABLE flutter optimization method requires a formulation that integrates the contributing analysis disciplines so that the redesign objectives may be attained efficiently and accurately. To accomplish these aims the structural model, the coordinate system, the dynamic representation, the design variables, and the optimization method must be compatible.

The appearance of publications concerned with dynamic optimization of structures indicates an increasing interest in this topic. Turner[1] approached the flutter problem with a method that proportioned structural members so that a specified vibration frequency assumed a given value. The structure attained its required eigenvalues with minimum mass. Other researchers[2-6] have investigated various optimization problems concerned with natural frequencies of structures.

Turner[7] developed a more realistic flutter optimization technique by incorporating aerodynamic forces and the flutter equations into the formulation. Lagrange extremization was used for seeking the configuration of minimum mass. Other researchers[8,9] developed computerized preliminary design programs for considering flutter and also other requirements such as strength and performance. Rudisill and Bhatia[10] developed search procedures using gradient methods. The method was applied to the design of a box beam for a rectangular lifting surface.

In general, resizing a structural component alters the flutter speed and also changes structural "optimality" or efficiency in utilizing structural weight for preventing flutter. The optimization method presented here calculates the gradient of total weight with respect to the variable structural components as the flutter speed remains fixed. It is anticipated that this weight gradient algorithm will be especially convenient when used iteratatively with a method for increasing flutter speed such as the velocity gradient of Ref. 10.

Derivation

With normal mode deflections used as generalized coordinates, the associated unsteady aerodynamic forces $[Q]$ may be calculated with an appropriate aerodynamic theory. The flutter characteristics of the structure are then specified by the following neutral stability equation.

$$([K] - \omega^2[M] - \omega^2[Q])\{q\} = \{0\} \tag{1}$$

Matrix $[K]$ is the generalized stiffness, $[M]$ is the generalized inertia, ω is the flutter frequency, and $\{q\}$ is the complex generalized coordinate vector.

The generalized stiffness and inertia terms are expressed in linear form as

$$[K] = [K^O] + \sum_{j=1}^{n} m_j [K^j] \tag{2}$$

Presented at the AIAA/ASME/SAE 14th Structures, Structural Dynamics, and Materials Conference, Williamsburg, Va., March 20–22; submitted March 29, 1973; revision received November 21, 1973.

Index categories: Aeroelasticity, Structural Design, Optimal.

*Senior Engineer, Structural Dynamics, Convair Aerospace Div.

$$[M] = [M^O] + \sum_{j=1}^{n} m_j \, [M^j] \tag{3}$$

Matrices $[K^{0}]$ and $[M^{0}]$ represent all the structure which is fixed in size. Each m_j, although normally used with units of weight, is called a variable mass which may be resized to satisfy flutter requirements. An m_j represents a portion of structure which contributes both stiffness and inertia with respect to the flutter mechanism. It may be idealized by one or, as in the examples to be presented here, a number of finite elements and lumped weights. The $[K^j]$ and $[M^j]$ represent generalized stiffness and inertia per unit weight for variable mass j.

Equations (2) and (3) may be substituted into Eq. (1) to obtain

$$\left([K^O] - \omega^2[M^O] + \sum_{j=1}^{n} m_j([K^j] - \omega^2[M^j]) - \omega^2[Q]\right)\{q\} = \{0\} \tag{4}$$

The flutter stability equation is a complex eigenvalue relation whose real and imaginary components can be separated as two real conditions and used to evaluate eigenvalues of two real variables. The usual V-g flutter analysis method obtains and plots eigenvalues of structural damping and flutter velocity. The Rudisill and Bhatia approach[10] considers damping as zero, the n variable masses as independent variables, and the flutter frequency and velocity as the two dependent variables for which gradients are calculated.

The choice of quantities to select as invariant may be made to conform to optimization objectives and to what is computationally an advantage. The approach herein considers flutter frequency, flutter velocity, and zero damping as specified. Generalized stiffness, inertia, and aerodynamic forces are expressed in terms of mode coordinates which are retained unchanged during individual optimization cycles. Two of the n variable masses are considered dependent functions of the remaining n-2 masses. The neutral stability equations are used to evaluate partial derivatives of the 2 dependent masses with respect to the independent masses. The gradient of total structural weight is then formed. The structure may then be modified in the manner indicated by the gradient to predict lower weight configurations with the same flutter speed.

The coefficients of m_j and other terms may be combined appropriately in Eq (4) to form matrices $[A]$ and $[B^j]$

$$[A] = [K^O] - \omega^2[M^O] - \omega^2[Q] \tag{5}$$

$$[B^j] = [K^j] - \omega^2[M^j] \tag{6}$$

Equation (4) then simplifies to

$$\left([A] + \sum_{j=1}^{n} m_j \, [B^j]\right)\{q\} = \{0\} \tag{7}$$

With any two of the variable masses arbitrarily designated as the dependent masses m_u and m_v, Eq. (7) becomes

$$\left([A] + \sum_{j=1}^{n-2} m_j \, [B^j] + m_u \, [B^u] + m_v \, [B^v]\right) \{q\} = \{0\} \tag{8}$$

Derivatives of Eq. (8) with respect to each of the m_j's will be found. Since modes and reduced frequency are not changing, the $[A]$ and $[B^j]$ quantities are constant with respect to the partial differentiation. Differentiation yields

$$\left([B^j] + [B^u]\frac{\partial m_u}{\partial m_j} + [B^v]\frac{\partial m_v}{\partial m_j}\right)\{q\} + \left([A] + \sum_{j=1}^{n} m_j \, [B^j]\right)\left\{\frac{\partial q}{\partial m_j}\right\} = \{0\} \tag{9}$$

With the flutter eigenvalue a row eigenvector exists such that

$$\{p\}^T\left([A] + \sum_{j=1}^{n} m_j[B^j]\right) = \{0\}^T \tag{10}$$

Premultiplying Eq. (9) by $\{p\}^T$, using Eq. (10), and condensing terms yields

$$\{p\}^T \, [B^j] \, \{q\} + \{p\}^T \, [B^u] \, \{q\} \frac{\partial m_u}{\partial m_j} + \{p\}^T \, [B^v] \, \{q\} \frac{\partial m_v}{\partial m_j} = 0 \tag{11}$$

Equation (11) is a complex relation with all terms known except partial derivatives $\partial m_u/\partial m_j$ and $\partial m_v/\partial m_j$. Real and imaginary components may be separated and the 2 resulting simultaneous equations solved for $\partial m_u/\partial m_j$ and $\partial m_v/\partial m_j$. The resulting derivatives are found to equal

$$\frac{\partial m_u}{\partial m_j} = \frac{c_2c_6 - c_4c_5}{c_1c_4 - c_2c_3} \tag{12}$$

$$\frac{\partial m_v}{\partial m_j} = \frac{c_3c_5 - c_1c_6}{c_1c_4 - c_2c_3} \tag{13}$$

With $i = (-1)^{1/2}$, $\{p\}^T = \{p'\}^T + i\{p''\}^T$, and $\{q\} = \{q'\} + i\{q''\}$, terms $c_1 - c_6$ are evaluated as

$$c_1 = \{p'\}^T[B^u]\{q'\} - \{p''\}^T \, [B^u] \, \{q''\} \tag{14}$$
$$c_2 = \{p'\}^T[B^v]\{q'\} - \{p''\}^T \, [B^v] \, \{q''\} \tag{15}$$
$$c_3 = \{p'\}^T[B^u]\{q''\} + \{p''\}^T \, [B^u] \, \{q'\} \tag{16}$$
$$c_4 = \{p'\}^T[B^v]\{q''\} + \{p''\}^T \, [B^v] \, \{q'\} \tag{17}$$
$$c_5 = \{p'\}^T[B^j]\{q'\} - \{p''\}^T \, [B^j] \, \{q''\} \tag{18}$$
$$c_6 = \{p'\}^T[B^j]\{q''\} + \{p''\}^T \, [B^j] \, \{q'\} \tag{19}$$

Denoting the weight of the fixed structure as W^0, the total weight W of the structure equals

$$W = W^o + \sum_{j=1}^{n-2} m_j + m_u + m_v \tag{20}$$

Differentiating Eq. (20) yields the partial derivative of total structural weight

$$(\partial W/\partial m_j) = 1 + (\partial m_u/\partial m_j) + (\partial m_v/\partial m_j) \tag{21}$$

A partial derivative is calculated for each independent variable mass to obtain the gradient of total weight with specified flutter speed

$$\{\nabla W\} = \left\{\frac{\partial W}{\partial m_1}, \frac{\partial W}{\partial m_2}, \ldots, \frac{\partial W}{\partial m_{n-2}}\right\} \tag{22}$$

The structure may then be resized to obtain a ΔW total weight reduction by using the well known gradient projection

$$\{m_1, m_2, \ldots, m_{n-2}\}_{\text{new}} = \{m_1, m_2, \ldots, m_{n-2}\}_{\text{old}} - \frac{\Delta W}{\{\nabla W\}^T\{\nabla W\}}\{\nabla W\} \tag{23}$$

New eigenvalues for m_u and m_v corresponding to $\{m\}_{\text{new}}$ are calculated to satisfy the neutral stability equation.

Application

The main intent of this paper is to present the weight gradient. The over-all approach to the optimization of dynamic structures is the same as that discussed in many of the cited references and will be reviewed only briefly. The optimization proceeds in cycles. The structure is initially represented by its mode properties. To obtain these, the

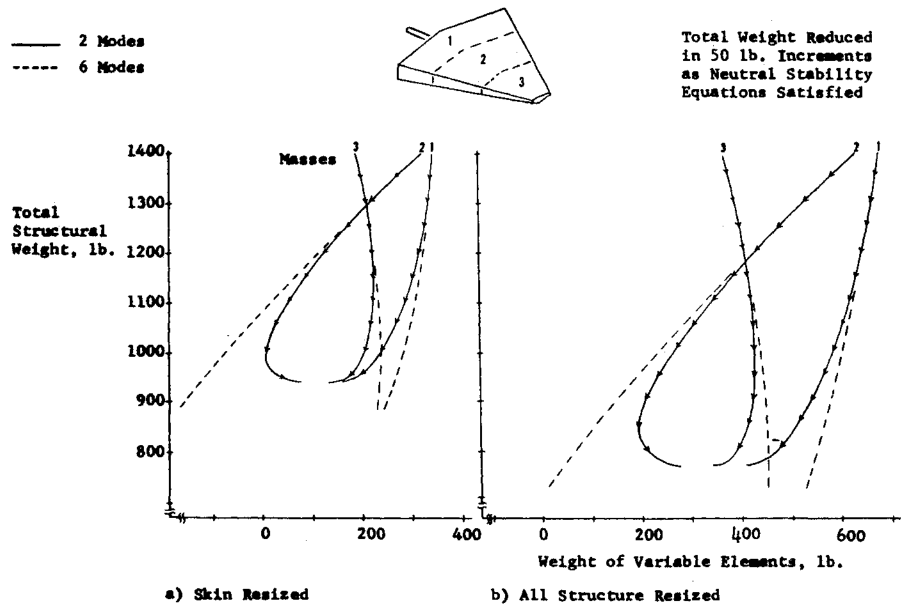

Fig. 1 Horizontal tail optimization.

structural stiffness matrix representing the fixed structure and the combined variable mass sizes is formed. Matrix operations "fix" and "eliminate" coordinates yielding a reduced stiffness matrix of selected coordinates which are usually deflections normal to the midplane of the aerodynamic surface. This matrix is inverted. With lumped weights appropriately representing the fixed and variable mass sizes, eigenvalue extraction obtains the frequency and shape of a suitable number of normal modes.

Using the mode deflections of the structural coordinates, an interpolation procedure then calculates corresponding deflections at selected locations which define the aerodynamic surface. Another procedure then calculates the unsteady aerodynamic forces associated with the normal modes for a number of reduced frequencies. The usual *V-g* method provides a flutter analysis. Numerical interpolation obtains the unsteady aerodynamic force matrix for the root of lowest flutter speed.

The $[K^{0}]$, $[M^{0}]$, $[K^{j}]$, $[M^{j}]$, ω, and $[Q]$ obtained from the cited procedures are functions of mode frequencies and shapes and remain constant until recalculated again for another cycle of optimization. For economy in nomenclature, the term "mode properties" will be used hereafter to refer to these quantities.

Based on the current mode properties, the gradient of structural weight is calculated by the equations of the previous section. The gradient obtained is the projection of the unrestricted weight gradient on the hyperplane tangent to the surface of constant flutter speed. It indicates the direction in which variable masses may be resized to obtain a structure of lower total weight with the same flutter speed. Equation (23) gives the optimal step to obtain a ΔW weight reduction. As the process of calculating gradients and taking steps is repeated, ideally a local extremum is obtained where the gradient equals zero. It has been found, however, that for all but the most simple structural idealizations, some of the variables rapidly approach values which are physically unrealistic. The objective is then an extremum constrained with respect to some variable masses. Some gradient components are zero and the variable mass values for the rest have progressed to unpermissible size limits, usually that of a strength design.

When a configuration that is extremal or otherwise adequate by a different rationale is obtained, new mode properties are calculated and another optimization cycle is begun. A local optimum may not always be the best choice for calculating the new set of mode properties if it represents a large deviation from the original configuration. Too drastic a variation may cause the flutter mechanism to change. In terms of a *V-g* plot, a different root may become dominant and cause a lower flutter speed than the original root.

For initiating the next optimization cycle in such cases, it is better to select a configuration of modest weight reduction that was previously obtained along the path to the extremum. The selection may be based on what is reasonable for the particular structure. A weight reduction of 15% from the initial configuration might often be appropriate. In short, modes should be recalculated often enough to adequately represent the changing structure. This process continues until the final optimum is found. Termination occurs when a configuration is obtained that is relatively unchanged from the one of the previous cycle.

Among the future additions planned for the weight gradient computer program are modifications concerning efficient step size, projections away from mass limit boundaries, and approximation techniques to estimate changes in mode properties between the times that the more expensive eigenvalue extractions are performed. At present, however, ΔW is an input quantity. Weight reduction continues until an extremum or a desired weight reduction, also input and usually the mentioned 15%, is obtained. As the size of a variable mass decreases and eventually reaches the strength design, it is temporarily eliminated as a design variable. Partial derivatives continue to be calculated for it. If calculations later indicate that it should move back into the acceptable design space, it is reinstated as a design variable.

Results

The weight gradient that has been introduced herein has as its objective a lower weight structure with the same flutter speed. Its effectiveness in reducing weight within one optimization cycle and the induced changes in flutter speed, flutter frequency, and modes are the appropriate features to demonstrate. Thus, all the results to be illustrated here are obtained using the initial set of normal modes. Additional stages of optimization would each be performed with updated modes. Results will be cited for a large all-movable horizontal tail. To illustrate the weight gradient and the nature of a typical application, a number of variations in idealization will be considered.

Figure 1 illustrates four applications of the weight gradient procedure. No constraints are placed on the sizes of any variable masses. The finite elements were grouped as indicated to form 3 variable masses. Aerodynamic forces

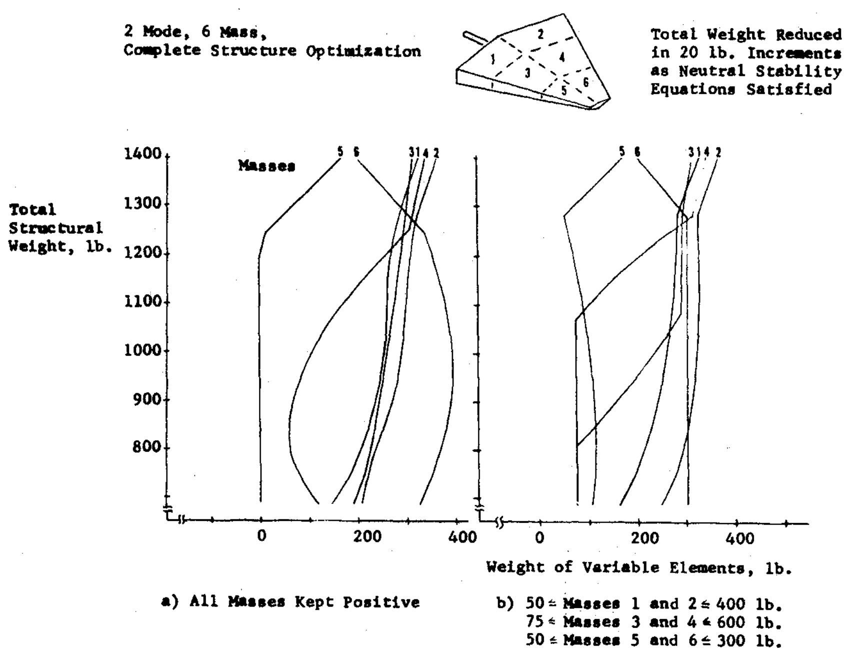

Fig. 2 Horizontal tail optimization with size constraints.

were calculated by a subsonic kernal function procedure.

In Fig. 1a only the finite elements of the composite skins were allowed to resize. In Fig. 1b the elements of the skin and all the internal structure were resized. Optimization was performed using 2 modes of vibration and also 6 modes of vibration. The 2-mode configurations are indicated by solid lines and the 6-mode configurations are indicated by dashed lines.

The vertical axis represents the total weight of the structure. The mass distributions of the initial configurations are located at the tops of the plots. The variable masses associated with the curves are identified by the numerals at the initial configurations. The total weight of the structure was reduced in 50 lb increments by the gradient procedure. The consecutive lower weight configurations are represented by the downward progression of arrowheads. The horizontal axis represents the weights of the individual masses. A mass that is becoming larger moves to the right. Every configuration satisfies the neutral stability equation and could be used for the next cycle of optimization.

The 2-mode cases bottom out and stop. These terminal points are extrema with zero gradients. The classical Lagrange optimization method of Turner,[7] when applied to this structure for comparison, also obtained these same extrema. Optimums of this type, although interesting, will be usable in only a small percentage of applications. It has been found that they generally represent large unrealistic deviations from the original structures. As discussed in the previous section, an earlier configuration along the path is a better choice for the next cycle. The 6-mode curves have shapes analogous to the 2-mode curves but with much lower extrema.

It is noted that the idealization with all the structure being resized produced a lower weight optimum than the one obtained by skin resizing. This result agrees with intuition since more structure was being modified to satisfy flutter requirements. The 6-mode curves are parallel to the 2-mode curves initially and then deviate from them. This also agrees with intuition since one would expect that eventually a different combination of masses would be required to satisfy the 6-mode flutter equations.

Figure 2 illustrates applications with constraints on the sizes of 6 variable masses. In Fig. 2a masses are kept greater than limit sizes of zero. In Fig. 2b variable masses are kept between upper and lower bounds. Masses 6, 4, and 3 reached limit values in that order. These masses would have been free to move from limit values back into the acceptable design region if required to by the continuing optimization.

The change in mode shapes and frequencies caused by resizing the structure is of interest. Properties will be compared for the original structure and two resized structures. Table 1 illustrates mode characteristics of 1) the original horizontal tail, 2) a configuration obtained from a 2-mode, 3 variable mass, skin optimization, and 3) a configuration obtained from a 6-mode, 3 variable mass, entire structure optimization. Configurations of 15% weight reduction for both optimized structures are compared. The characteristics of the resized structures are obtained from complete finite element, mode, aerodynamic, and flutter analyses.

The flutter speed of a structure generally increases as the frequencies of the vibration modes increase. The 2 mode optimization utilizes the first bending and first torsion modes. The objective of trial and error flutter modification is usually to raise and separate the frequencies of these modes. Table 1 shows that the 2 mode optimization does exactly this. The first two frequencies are increased and the remaining 4 frequencies drop sharply. This would apparently indicate that the structure was being modified selectively to increase the mode frequencies used in the optimization at the expense of the other modes which were not represented. The flutter speed decreases 4.5 knots with a 2 mode flutter analysis and 16 knots with a 6 mode flutter analysis.

The 6-mode optimization similarly modifies the frequencies in a manner that is appropriate to the modes used in its calculations. The magnitudes of the generalized coordinates $\{q\}$ for the flutter condition of the original structure are illustrated in Table 1. These values indicate the contributions of the respective modes to the steady state flutter oscillations. The largest values indicate the modes which are most significant at the flutter condition. An effective structural modification would increase the frequencies of the most significant modes.

For the 6-mode optimization it is observed that the bending and torsion frequencies are again increased as in the 2-mode optimization. The 6th mode has the 3rd largest generalized coordinate value and its frequency is increased slightly whereas it decreased considerably for the 2-mode optimization. Frequencies 3–5, which have the smallest generalized coordinate values are decreased but not nearly as much as in the 2-mode case where these

Table 1 Properties of optimized horizontal tail

Idealization	$\|\{q\}\|$ Modes 1–6	Frequencies Modes 1–6	Flutter speed 2 mode analysis	Flutter speed 6 mode analysis	Flutter frequency 2 mode analysis	Flutter frequency 6 mode analysis
Original structure	17.2	52.74	676.5	667.8	71.57	71.39
(actual values cited)	16.4	96.37				
units: freq rad/sec	0.57	237.84				
speed kts	0.27	298.87				
	0.23	390.72				
	1.00	530.97				
Optimized structure		+0.65	−4.5	−16.	−3.15	−3.20
2 mode, 3 mass,		+2.60				
skin optimization		−19.58				
15% weight reduction		−26.30				
(net changes cited)		−68.88				
		−14.91				
Optimized structure		+0.96	+1.5	−4.5	−0.75	−0.75
6 mode, 3 mass, all		+2.94				
component optimization		−7.25				
15% weight reduction		−7.47				
(net changes cited)		−27.14				
		+0.12				

modes were not present. The 2-mode optimization evidently resizes the structure to the advantage of a 2-mode flutter mechanism while 6-mode optimization resizes the structure for a 6-mode flutter mechanism. The flutter speed decreased 4.5 knots.

Of the idealizations considered, a 6-mode optimization with 6-mode flutter analysis was the most realistic mathematical representation of the actual horizontal tail. A 15% weight reduction was obtained with a decrease in flutter speed of less than 1%. The composite horizontal tail was represented by 76 finite elements with 260 node coordinates. Included among these are 29 anisotropic panel elements. Six normal modes were calculated. Flutter analysis with subsonic kernal function aerodynamics was performed using 20 reduced frequencies. The flutter analysis was repeated with very closely spaced reduced frequencies in order to determine accurately the flutter characteristics cited here. Neglecting setup time, each calculation of these mode dependent quantities typically requires about 10 minutes of CPU time on an IBM 370, Model 155 computer. A 6 mass, 6-mode problem with upper and lower constraints on masses typically requires about 5 seconds of CPU time for all the gradient calculations associated with one set of modes.

Conclusion

Equations have been presented for direct calculation of the gradient of total structural weight with respect to variable structural parameters as the flutter speed remains constant. In applications thus far, the method has been efficient in reducing weight while retaining flutter speed without frequent recalculation of normal modes of vibration. It is anticipated that this weight gradient algorithm will be especially convenient when used iteratively with a gradient method for increasing flutter speed.

References

[1]Turner, M. J., "Design of Minimum Mass Structures with Specified Natural Frequencies," *AIAA Journal,* Vol. 3, No. 3, March 1967, pp. 406–412.

[2]Taylor, J. E., "Minimum Mass Bar for Axial Vibration at Specified Natural Frequency," *AIAA Journal,* Vol. 5, No. 10, Oct. 1967, pp. 1911–1913.

[3]Zarghamee, M. S., "Optimum Frequency of Structures," *AIAA Journal,* Vol. 6, No. 4 April 1968, pp. 749–750.

[4]McCart, B. R., Haug, E. J., and Streeter, J. D., "Optimal Design of Structures with Constraints on Natural Frequency," AIAA Structural Dynamics and Aeroelasticity Specialist Conference, AIAA, New York, 1969.

[5]Rubin, C. P., "Dynamic Optimization of Complex Structures," AIAA Structural Dynamics and Aeroelasticity Specialist Conference, AIAA, New York, 1969.

[6]Johnson, J. R. and Warren, D. S., "Structural Optimization of a Supersonic Horizontal Stabilizer," 29th Meeting of the Structures and Materials Panel Advisory Group for Aerospace Research and Development, Istanbul, Turkey, Oct. 1969.

[7]Turner, M. J., "Optimization of Structures to Safisty Flutter Requirement," *AIAA Journal,* Vol. 7, No. 5, May 1969, pp. 945–951.

[8]Stroud, W. J., Dexter, C. B. and Stein, M., "Automated Preliminary Design of Simplified Wing Structures to Satisfy Strength and Flutter Requirements," TN D-6534, Dec. 1971. NASA.

[9]Tripplett, W. E. and Ising, K. D., "Computer Aided Stabilator Design Including Aeroelastic Constraints," *Journal of Aircraft,* Vol. 8, No. 7, July 1971, pp. 554–561.

[10]Rudisill, C. S. and Bhatia, K. G., "Optimization of Complex Structures to Satisfy Flutter Requirements," *AIAA Journal,* Vol. 9, No. 8, Aug. 1971, pp. 1487–1491.